



Cite this: *RSC Adv.*, 2025, 15, 39028

# Design, synthesis and acaricidal activity of tetrahydrothiophene derivatives against *Psoroptes cuniculi*

Dongdong Chen,<sup>ID</sup>\*<sup>a</sup> Yan Wang,<sup>ba</sup> Yujun Wu,<sup>ba</sup> Qiaoqiao Yu,<sup>a</sup> Yunhan Wang,<sup>a</sup> Junyao Zheng,<sup>a</sup> Zhong Ying<sup>c</sup> and Changhui Hou<sup>c</sup>

A series of sulfur-containing five-membered heterocycles were devised and prepared, with substituted chalcones and elemental sulfur acting as precursors. They were subsequently oxidized into the relevant tetrahydrothiophene sulfone derivatives. *In vitro* assessments were carried out to gauge the acaricidal activity of all 44 synthesized compounds against *Psoroptes cuniculi*. Based on mass concentration and molar concentration, 16 and 14 compounds, respectively, exhibited significantly superior acaricidal activity compared to the commercial drug ivermectin. Structure–activity relationship (SAR) studies revealed that the sulfone group was an essential structural motif for the acaricidal activity. When halogens and strong electron-withdrawing groups were introduced at the 3- and 5-positions of the benzene ring, the activity was significantly boosted via electronic effects and spatial compatibility. Molecular docking experiments confirmed that tetrahydrothiophene sulfone derivatives can form multiple interactions with the active pocket of acetylcholinesterase (AChE).

Received 26th July 2025  
Accepted 8th October 2025

DOI: 10.1039/d5ra05421d

rsc.li/rsc-advances

## 1 Introduction

Mange, a common parasitic disease, occurs when mites infest the epidermis of animals.<sup>1</sup> It is widespread in livestock and poultry farming globally, posing a persistent threat to animal health and the development of the breeding industry.<sup>2,3</sup> Among them, *Psoroptes cuniculi*, as an important group of mites, primarily parasitizes in the ear canals of animals.<sup>4</sup> It damages the host's epidermal tissues through its specialized mouthparts and movement patterns, and can infect not only common livestock and poultry such as rabbits, goats, horses, buffaloes, and sheep, but also spread among wild animal populations, creating a potential risk of cross-species transmission.<sup>5–7</sup> Animals infected with *Psoroptes cuniculi* reduce their food intake due to pruritus-induced stress, resulting in a significant decrease in body weight. For fur-bearing animals, the quality of their leather deteriorates severely due to skin damage, leading to a substantial reduction in economic value.<sup>8,9</sup> Breeding females may experience reduced conception rates, miscarriages, or weak offspring due to poor physical condition. In extreme cases, severe infestations can cause systemic infections or secondary bacterial infections, which may directly result in animal death.<sup>10</sup> Mange caused by *Psoroptes cuniculi* has become

a global animal epidemic and remains one of the key bottlenecks restricting the sustainable development of animal husbandry.<sup>11</sup>

In practical control measures, chemical drugs remain the primary means for managing animal mange, with commonly used agents including organochlorines, organophosphates, pyrethroids, and avermectins.<sup>12</sup> However, long-term and extensive application has led to several intractable issues: mites have gradually developed drug resistance under selective pressure from these chemicals; drug residues in animal bodies can infiltrate the human food chain, thereby creating potential hazards for human health;<sup>13</sup> and when excreted into the

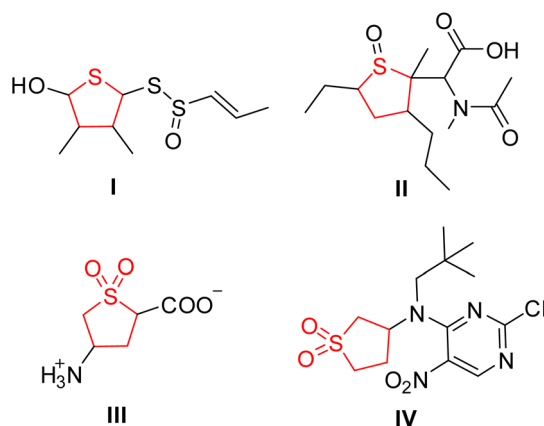


Fig. 1 Compounds containing tetrahydrothiophene ring.

<sup>a</sup>Department of Chemical and Material Engineering, Lyuliang University, Lvliang 033001, China

<sup>b</sup>School of Chemistry and Chemical Engineering, Shanxi University, Taiyuan 030006, China

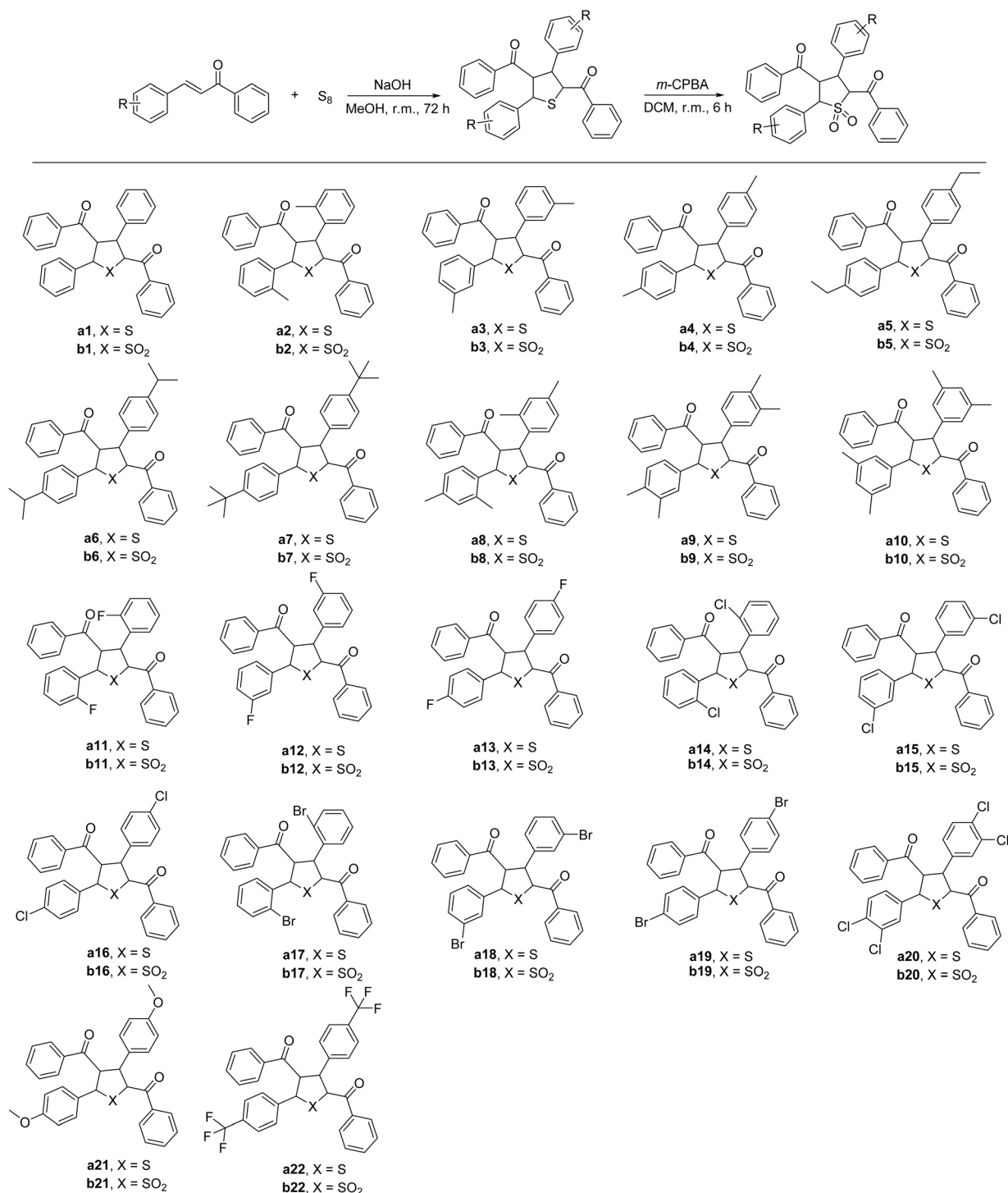
<sup>c</sup>Nanchang Institute of Science and Technology, Nanchang 330000, China



environment, these drugs may disrupt ecological balance.<sup>14–17</sup> Thus, the development of novel anti-mite agents with high efficacy, low toxicity, and environmental friendliness has become an urgent need in the current field of animal parasitic disease control.

Sulfur-containing compounds occupy a crucial position in nature and life sciences due to their unique chemical structures and physicochemical properties, particularly exhibiting

irreplaceable value in natural products,<sup>18,19</sup> development,<sup>20,21</sup> and bioactive molecule research.<sup>22,23</sup> As an important class of sulfur-containing five-membered heterocyclic compounds, tetrahydrothiophene derivatives have attracted increasing attention in bioactivity studies in recent years, demonstrating diverse biological activities such as antioxidant, antiviral, anti-bacterial and hypoglycemic effects.<sup>24–28</sup> The 3,4-dimethylthiolane natural product isolated from onions (Fig. 1,



Scheme 1 Structures of tetrahydrothiophene derivatives.



compound **I**) exerts antiplatelet coagulation effects by inhibiting cyclooxygenase-1 (COX-1), with efficacy far superior to that of aspirin.<sup>29</sup> Highly substituted thiolane ring identified from *Eupolymania nebulosa* (Fig. 1, compound **II**) showed excellent antioxidant activity.<sup>30</sup> Tetrahydrothiophene-based GABA analogue (Fig. 1, compound **III**) can specifically inactivate  $\gamma$ -aminobutyric acid aminotransferase, exhibiting significant potential in anti-Alzheimer's disease.<sup>31</sup> Additionally, the thiophene sulfone-substituted pyrimidine derivatives (Fig. 1, compound **IV**) have emerged as potential anticancer agents by forming covalent bonds with Pin1.<sup>32</sup> These research findings have confirmed the enormous application potential of tetrahydrothiophene derivatives as bioactive molecules.

In this study, a series of tetrahydrothiophene derivatives (**a1**–**a22**) were designed and synthesized using substituted chalcones and elemental sulfur as starting materials, which were further oxidized to obtain the corresponding sulfone derivatives (**b1**–**b22**). *In vitro* assays were used to explore the acaricidal efficacy of target compounds on *Psoroptes cuniculi*. Their structure–activity relationship (SAR) was systematically investigated, and preliminary analysis of the potential mechanism of action was conducted using molecular docking technology.

## 2 Results and discussion

### 2.1 Synthesis and structures of tetrahydrothiophene derivatives

In Scheme 1, a series of sulfur-containing heterocyclic compounds, 3,5-diaryltetrahydrothiophene derivatives (**a1**–**a22**), were successfully constructed using substituted chalcones and sulfur powder as starting materials, with yields ranging from 32% to 91%. Subsequently, the above-mentioned tetrahydrothiophene derivatives were oxidized using *m*-chloroperoxybenzoic acid (*m*-CPBA) to obtain the corresponding sulfone derivatives (**b1**–**b22**), and this step achieved high yields of 92% to 98%. Among the forty-four synthesized tetrahydrothiophene derivatives, seven compounds (**a1**, **a2**, **a4**, **a15**, **a16**, **a19**, **a21**) are known, while the remaining thirty-seven are new compounds.

Structural characterization of all forty-four synthesized tetrahydrothiophene derivatives relied on <sup>1</sup>H NMR, <sup>13</sup>C NMR, and HRMS. For compound **b17**, X-ray single-crystal diffraction further confirmed its spatial configuration (Fig. 2).<sup>33</sup> <sup>1</sup>H NMR, <sup>13</sup>C NMR, HRMS data, and X-ray diffraction results for these derivatives are detailed in the SI.

### 2.2 Acaricidal activity *in vitro*

Data on the *in vitro* acaricidal effects of compounds against *P. cuniculi* were compiled in Table 1. Ivermectin, a clinically commonly used acaricidal drug, was selected as the reference control, while a blank control without drugs was used to calibrate the baseline for activity evaluation, ensuring the reliability and accuracy of the test results. At the relatively high concentration of 0.5 mg mL<sup>−1</sup>, all compounds exhibited acaricidal activity to varying degrees, indicating that this class of structures has a potential basis for anti-mite effects. Notably, the

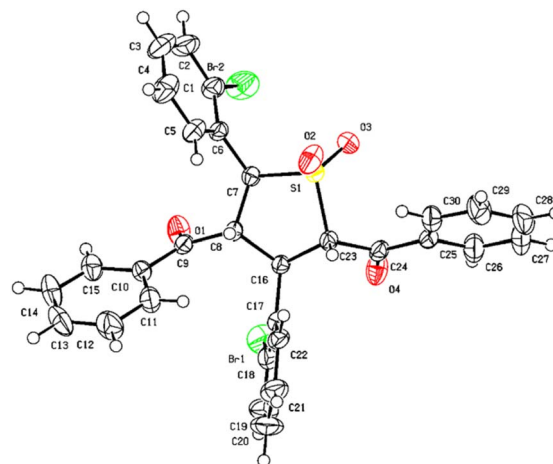


Fig. 2 Crystal structure of compound **b17** (CCDC 2468721).

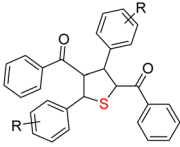
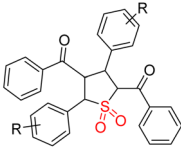
acaricidal activity of sulfone derivatives (**b1**–**b22**) was significantly superior to that of their corresponding parent tetrahydrothiophene compounds (**a1**–**a22**), suggesting that the modification of the oxidation state of sulfur atoms plays a key regulatory role in enhancing activity. Among the forty-four synthesized compounds, twenty-five compounds (**a4**, **a12**–**a20**, **a22**, **b2**–**b4**, **b11**–**b20**, **b22**) showed excellent acaricidal activity, with mite mortality rates exceeding 80%, which were superior to that of the reference control ivermectin (76.7%). Ten compounds (**a19**, **a22**, **b12**, **b13**, **b15**, **b16**, **b18**–**b20**, **b22**) achieved 100% mortality, and another five compounds (**a16**, **a20**, **b11**, **b14**, **b17**) showed mortality rates exceeding 95%, approaching complete lethal efficacy. For compounds with activity superior to ivermectin, the test concentration was further reduced to 0.25 mg mL<sup>−1</sup> for activity verification. Sixteen compounds (**a13**, **a16**, **a20**, **a22**, **b4**, **b11**–**b20**, **b22**) still exhibited higher activity than ivermectin (65%) at this concentration. Among them, six compounds (**b13**, **b16**, **b18**–**b20**, **b22**) achieved 100% lethality, and two compounds (**b12**, **b15**) showed mortality rates of 98.3% and 96.7%, respectively, approaching complete killing efficacy.

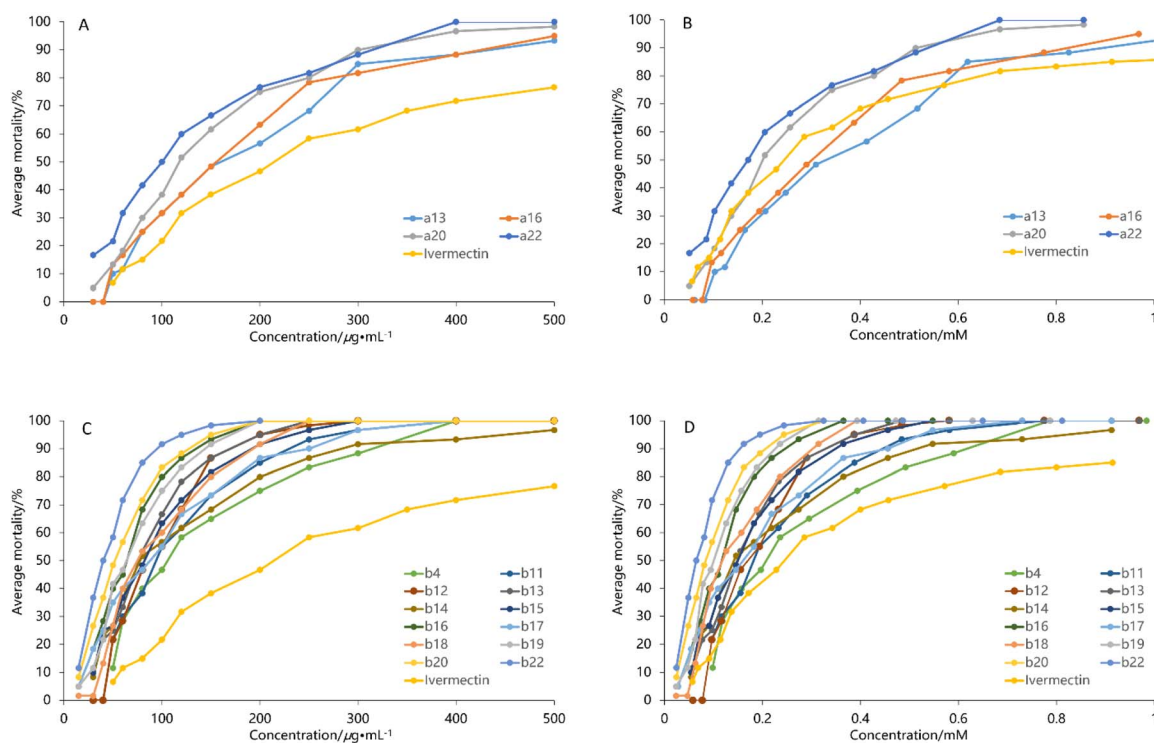
For the 16 compounds (**a13**, **a16**, **a20**, **a22**, **b4**, **b11**–**b20**, **b22**) initially screened at 0.25 mg mL<sup>−1</sup> — which showed *in vitro* acaricidal potency against *P. cuniculi* exceeding reference drug ivermectin (Table 1) — we subsequently determined their median lethal concentration (LC<sub>50</sub>) and time (LT<sub>50</sub>) to systematically characterize acaricidal efficacy. Fig. 3A and B illustrate mite mortality trends for four series a compounds at different test concentrations (molar or mass) with uniform 24 h treatment. Fig. 3C and D correspondingly show the mortality dynamics of twelve compounds in series b. Fig. 4A and B illustrate mortality trends for series a/b compounds at 4.5 mM (fixed concentration) with varied treatment durations.

At the condition of the same mass concentration, all four selected compounds in series a exhibited superior acaricidal activity against *Psoroptes cuniculi* compared to ivermectin (Fig. 3A). However, when evaluated by molar concentration, only compounds **a20** and **a22** achieved or exceeded the activity



Table 1 Acaricidal activity of tetrahydrothiophene derivatives

							
		Mortality % (mean $\pm$ S.D.)				Mortality % (mean $\pm$ S.D.)	
No.	R	0.5 mg mL <sup>-1</sup>	0.25 mg mL <sup>-1</sup>	No.	R	0.5 mg mL <sup>-1</sup>	0.25 mg mL <sup>-1</sup>
a1	H	56.7 $\pm$ 5.2	ND	b1	H	73.3 $\pm$ 5.2	40.0 $\pm$ 6.3
a2	2-Me	51.7 $\pm$ 4.1	ND	b2	2-Me	81.7 $\pm$ 7.5	48.3 $\pm$ 7.5
a3	3-Me	66.7 $\pm$ 5.2	ND	b3	3-Me	86.7 $\pm$ 5.2	55.0 $\pm$ 5.5
a4	4-Me	83.3 $\pm$ 5.2	45.0 $\pm$ 5.5	b4	4-Me	91.7 $\pm$ 4.1	83.3 $\pm$ 4.1
a5	4-Et	50.0 $\pm$ 0.0	ND	b5	4-Et	61.7 $\pm$ 4.1	ND
a6	4-iPr	45.0 $\pm$ 5.5	ND	b6	4-iPr	58.3 $\pm$ 4.1	ND
a7	4-iBu	33.3 $\pm$ 5.2	ND	b7	4-iBu	53.3 $\pm$ 8.2	ND
a8	2,4-diMe	51.7 $\pm$ 7.5	ND	b8	2,4-diMe	60.0 $\pm$ 6.3	ND
a9	3,4-diMe	23.3 $\pm$ 5.2	ND	b9	3,4-diMe	51.7 $\pm$ 4.1	ND
a10	3,5-diMe	33.3 $\pm$ 5.2	ND	b10	3,5-diMe	48.3 $\pm$ 4.1	ND
a11	2-F	76.7 $\pm$ 5.2	51.7 $\pm$ 9.8	b11	2-F	95.0 $\pm$ 5.5	93.3 $\pm$ 5.2
a12	3-F	90 $\pm$ 0.0	60.0 $\pm$ 6.3	b12	3-F	100.0 $\pm$ 0.0	98.3 $\pm$ 4.1
a13	4-F	93.3 $\pm$ 5.2	68.3 $\pm$ 4.1	b13	4-F	100.0 $\pm$ 0.0	100.0 $\pm$ 0.0
a14	2-Cl	78.3 $\pm$ 4.1	51.7 $\pm$ 4.1	b14	2-Cl	96.7 $\pm$ 5.2	81.7 $\pm$ 7.5
a15	3-Cl	85.0 $\pm$ 5.5	61.7 $\pm$ 4.1	b15	3-Cl	100.0 $\pm$ 0.0	96.7 $\pm$ 5.2
a16	4-Cl	95.0 $\pm$ 5.5	78.3 $\pm$ 4.1	b16	4-Cl	100.0 $\pm$ 0.0	100.0 $\pm$ 0.0
a17	2-Br	81.7 $\pm$ 4.1	48.3 $\pm$ 9.8	b17	2-Br	98.3 $\pm$ 4.1	88.3 $\pm$ 4.1
a18	3-Br	91.7 $\pm$ 4.1	56.7 $\pm$ 8.2	b18	3-Br	100.0 $\pm$ 0.0	100.0 $\pm$ 0.0
a19	4-Br	100.0 $\pm$ 0.0	60.0 $\pm$ 0.0	b19	4-Br	100.0 $\pm$ 0.0	100.0 $\pm$ 0.0
a20	3,4-diCl	98.3 $\pm$ 4.1	71.7 $\pm$ 4.1	b20	3,4-diCl	100.0 $\pm$ 0.0	100.0 $\pm$ 0.0
a21	4-OMe	26.7 $\pm$ 5.2	ND	b21	4-OMe	53.3 $\pm$ 5.2	ND
a22	4-CF <sub>3</sub>	100.0 $\pm$ 0.0	81.7 $\pm$ 4.1	b22	4-CF <sub>3</sub>	100.0 $\pm$ 0.0	100.0 $\pm$ 0.0
Ivermectin		76.7 $\pm$ 5.2	65.0 $\pm$ 5.5	Blank		0.0 $\pm$ 0.0	0.0 $\pm$ 0.0

Fig. 3 Impact of concentrations on anti-*P. cuniculi* acaricidal efficacy (24 h). Series a (A and B), series b (C and D).

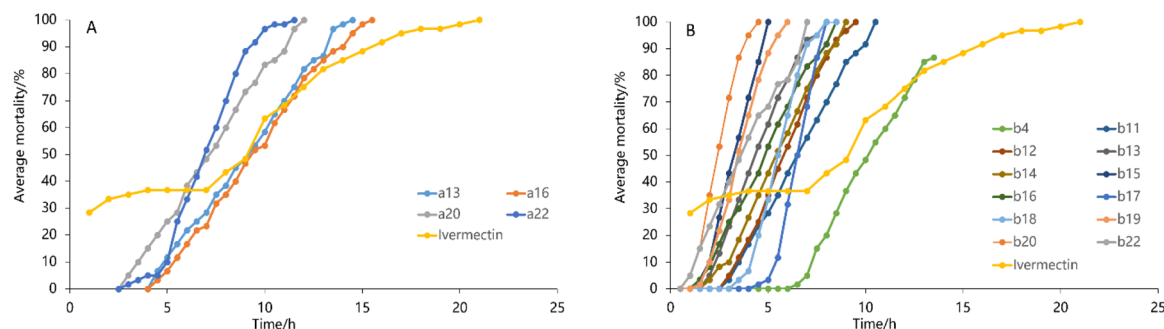


Fig. 4 Impact of treatment times on anti-*P. cuniculi* acaricidal efficacy (4.5 mM). Series a (A), series b (B).

level of ivermectin across all tested concentrations (Fig. 3B). This variation arises from differing concentration scaling methods: test compounds' molecular weights (484–586) are far lower than ivermectin (875). Therefore, at the same mass concentration, the molar concentration of the test compounds was actually higher, which accounts for their better performance when characterized by mass concentration. In sharp contrast to series **a**, for the twelve compounds in series **b**, regardless of whether the concentration was expressed in mass concentration or molar concentration, all their mortality curves lie above that of ivermectin's, indicating series **b** compounds outperform ivermectin in acaricidal efficacy and have greater anti-mite potential.

At a concentration of 4.5 mM, among the four compounds in series **a**, compounds **a20** and **a22** generally exhibited higher sensitivity to treatment time than ivermectin, while **a13** and **a16** showed time sensitivity similar to that of ivermectin. Notably, the dose–response curves of compounds **a13** and **a16** displayed a high degree of similarity (Fig. 4A), suggesting that they may share a similar mode of action. For the twelve compounds in

series **b**, in most cases (eleven compounds), their sensitivity to treatment time was higher than that of ivermectin, with only compound **b4** showing slightly lower time sensitivity than ivermectin. This further confirms the overall superior acaricidal kinetic characteristics of series **b** compounds.

LC<sub>50</sub> data for the test compounds are summarized in Table 2. When evaluated by mass concentration, the LC<sub>50</sub> values of all test compounds were lower than that of ivermectin (219.2 µg mL<sup>-1</sup>), indicating that their acaricidal activity was superior to ivermectin, which was consistent with the preliminary screening results. The relative activity (RA) of these compounds was 1.45–5.74 fold that of ivermectin. Among them, **b22** showed the highest acaricidal potency: LC<sub>50</sub> at 38.2 µg mL<sup>-1</sup> and RA 5.74-fold of ivermectin. In contrast, **a13** exhibited lower activity (LC<sub>50</sub>: 150.9 µg mL<sup>-1</sup>; RA: 1.45-fold of ivermectin). However, when LC<sub>50</sub> was characterized by molar concentration, only fourteen of the above compounds showed acaricidal activity superior to ivermectin, and the other two compounds (**a13**, **a16**) had higher LC<sub>50</sub> values than ivermectin. Moreover, the relative activity (RA) of all compounds was lower than the results calculated by mass concentration. This phenomenon stems from test compounds' molecular weights (484–586) being far lower than ivermectin's (875). Compared to mass concentration, molar concentration provided a better reflection of the interactions between a compound and its biological target, thereby enabling a more accurate interpretation of the structure–activity relationship (SAR).

The LT<sub>50</sub> of the test compounds was listed in Table 3. Thirteen compounds outperformed ivermectin in acaricidal kinetics, with LT<sub>50</sub> at 2.2–6.8 h and RA 1.26–3.19-fold. Only **a13**, **a16**, and **b4** showed slower rates. Compound **b20** exhibits the fastest action: LT<sub>50</sub> = 2.2 h and RA = 3.91-fold of ivermectin, demonstrating strong rapid-acting efficacy.

Given that chalcone derivatives are widely distributed in nature, exhibit diverse biological activities (such as antibacterial, anti-inflammatory, antitumor, and antioxidant properties), and have well-documented safety profiles, and considering that the tetrahydrothiophene derivatives in this study are constructed using chalcone as a key building block—with a molecular structure that can be viewed as two chalcone molecules linked *via* a sulfur atom—we reasonably infer that the newly synthesized tetrahydrothiophene derivatives will also possess favorable safety characteristics.

Table 2 24 h LC<sub>50</sub> values of the compounds

Compound	LC <sub>50</sub>		RA <sup>a</sup>
	µg mL <sup>-1</sup>	mmol L <sup>-1</sup>	
<b>a13</b>	150.9	0.31	1.45 (0.81)
<b>a16</b>	141.0	0.27	1.55 (0.93)
<b>a20</b>	117.9	0.20	1.86 (1.25)
<b>a22</b>	99.2	0.17	2.21 (1.47)
<b>b4</b>	108.9	0.21	2.01 (1.19)
<b>b11</b>	91.7	0.18	2.39 (1.39)
<b>b12</b>	83.5	0.16	2.63 (1.56)
<b>b13</b>	72.4	0.14	3.03 (1.79)
<b>b14</b>	88.7	0.16	2.47 (1.56)
<b>b15</b>	75.3	0.14	2.91 (1.79)
<b>b16</b>	56.3	0.10	3.89 (2.50)
<b>b17</b>	74.7	0.12	2.93 (2.08)
<b>b18</b>	79.8	0.13	2.75 (1.92)
<b>b19</b>	64.0	0.10	3.43 (2.50)
<b>b20</b>	48.5	0.08	4.52 (3.13)
<b>b22</b>	38.2	0.06	5.74 (4.17)
Ivermectin	219.2	0.25	1.00 (1.00)

<sup>a</sup> Relative activity = LC<sub>50</sub>(ivermectin)/LC<sub>50</sub>(test compound).





Table 3 4.5  $\mu\text{mol mL}^{-1}$   $\text{LC}_{50}$  values of the compounds

Compound	$\text{LT}_{50}$ (h)	$\text{RA}^a$
<b>a13</b>	8.7	0.99
<b>a16</b>	9.0	0.96
<b>a20</b>	6.8	1.26
<b>a22</b>	6.8	1.26
<b>b4</b>	10.0	0.86
<b>b11</b>	6.2	1.39
<b>b12</b>	5.5	1.56
<b>b13</b>	4.1	2.10
<b>b14</b>	5.1	1.69
<b>b15</b>	3.2	2.69
<b>b16</b>	4.4	1.95
<b>b17</b>	6.5	1.32
<b>b18</b>	5.4	1.59
<b>b19</b>	3.3	2.61
<b>b20</b>	2.2	3.91
<b>b22</b>	3.4	2.53
Ivermectin	8.6	1.00

<sup>a</sup> Relative activity =  $\text{LT}_{50}(\text{ivermectin})/\text{LT}_{50}(\text{test compound})$ .

### 2.3 Structure–activity relationship

By analyzing compound structures in Scheme 1, alongside preliminary screening activity data and  $\text{LC}_{50}/\text{LT}_{50}$  parameters from Tables 1–3, this study reveals clear structure–activity relationship (SAR) rules. For the tetrahydrothiophene core, sulfone derivatives (series **b**, formed by oxidation) exhibit significantly enhanced acaricidal activity compared with non-oxidized tetrahydrothiophene derivatives (series **a**). This phenomenon fully indicates that the introduction of the sulfonyl group can effectively improve the acaricidal activity of the compounds. Similar regulatory effects of sulfur oxidation states on activity have also been reported in other sulfur-containing heterocyclic compounds. The influence of the position and type of phenyl substituents on acaricidal activity presents complex yet ordered rules: compounds with unsubstituted phenyl rings (**a1**, **b1**) show basal activity, indicating that the parent structure already has a certain ability to bind to the target. The introduction of methyl groups (**a1** vs. **a2–a4**, **b1** vs. **b2–b4**) can enhance activity, and the potentiation effect of *para*-substitution is superior to that of *ortho*- and *meta*-substitution (**a2** vs. **a3** vs. **a4**, **b2** vs. **b3** vs. **b4**), suggesting the impact of steric hindrance on activity. Lengthening of alkyl chains (ethyl) or branching (isopropyl, *tert*-butyl) both lead to decreased activity (**a4** vs. **a5–a7**, **b4** vs. **b5–b7**), revealing strict selectivity for small molecule size in this region. The activity of polymethyl-substituted compounds (**a8–a10**, **b8–b10**) is weaker than that of monosubstituted ones, indicating that over-substitution may interfere with effective binding to the target. Compared with aliphatic hydrocarbon substituents, halogen substitution shows more significant enhancement of activity (**a1** vs. **a11–a19**, **b1** vs. **b11–b19**), following the order  $\text{Cl} > \text{Br} > \text{F}$ . Notably, the activity advantage of halogen substitution also follows the spatial distribution pattern of *para*- > *meta*- > *ortho*-. Combined with the synergistic enhancement effect of activity in polyhalogenated derivatives, this further confirms the requirement for spatial and electronic complementarity of the target binding pocket.

Studies on electronic effects show that electron-donating groups ( $-\text{OCH}_3$ ) significantly reduce activity (**a21**, **b21**), while strong electron-withdrawing groups ( $-\text{CF}_3$ ) exhibit the best potentiation effect (**a22**, **b22**). Among them, the compound with *para*-trifluoromethyl substitution (**b22**) shows the optimal acaricidal activity ( $\text{LC}_{50} = 38.2 \mu\text{g mL}^{-1}$ ,  $0.06 \text{ mmol L}^{-1}$ ), with an activity improvement of 5.74-fold (mass concentration) or 4.17-fold (molar concentration) compared with the reference control ivermectin. This result not only verifies the critical role of electronic effects in SAR but also provides an important basis for the design of subsequent highly active compounds.

### 2.4 Molecular docking analysis

Acetylcholinesterase (AChE), a pivotal enzyme for nerve conduction, ensures accurate signal transmission by specifically degrading neurotransmitter acetylcholine. Long recognized as a critical target for regulating insect and mite physiological activities,<sup>34</sup> this study uses molecular docking to explore how tetrahydrothiophene derivatives interact with AChE, aiming to clarify the target compounds' acaricidal mechanism.

The molecular docking results (Fig. 5) showed that the interaction between the less active 4-*tert*-butyl-substituted compound (**b7**) and the AChE receptor binding pocket was mainly dominated by weak interactions. Its aromatic ring bound to the amino acid residues in the pocket through non-

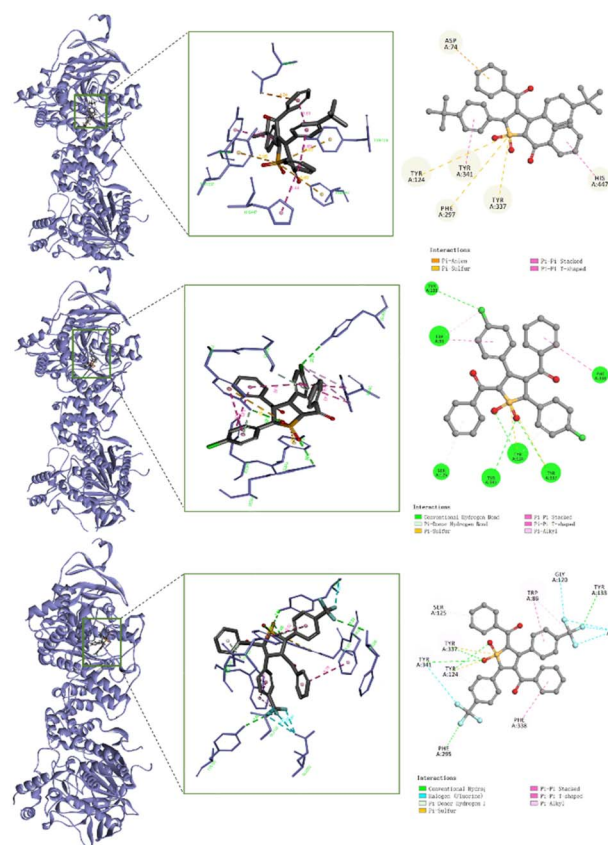


Fig. 5 Binding modes of compounds **b7**, **b16**, **b22** to AChE (PDB: 5DTI).



covalent interactions such as  $\pi\cdots\text{anion}$ ,  $\pi\cdots\text{sulfur}$ ,  $\pi\cdots\pi$  stacked, and  $\pi\cdots\pi$  T-shaped interactions, with a binding energy of  $-6.548\text{ kcal mol}^{-1}$ , and the overall molecular fit was not efficient. In contrast, the binding mode of the *para*-chloro-substituted compound (**b16**) with AChE was more optimized: in addition to binding through the above weak interactions, it could also form four strong hydrogen bonds with TyrA341, TyrA124, TyrA337, and TyrA133. The molecular fit was significantly improved, with a binding energy of  $-8.675\text{ kcal mol}^{-1}$ , showing better binding activity. The 4-trifluoromethyl-substituted compound (**b22**) exhibited more excellent binding characteristics: it formed five strong hydrogen bonds with PheA295, TyrA133, TyrA337, TyrA124, and TyrA341, and at the same time, its fluorine atoms formed five halogen bonds (fluorine bonds) with GlyA120, GluA202, and TyrA341, with a binding energy of  $-8.880\text{ kcal mol}^{-1}$ , achieving the highest fit with the receptor. The above molecular docking results were highly consistent with the *in vitro* activity evaluation results in Table 1, further verifying the structure–activity relationship between structural characteristics and biological activity.

## 3 Experimental

### 3.1 Materials and instruments

Reactions were monitored *via* thin-layer chromatography (TLC, GF<sub>254</sub> plates). Melting points (m.p.) were measured using an MP420 apparatus (Hanon Technologies, Jinan, China).  $^1\text{H}/^{13}\text{C}$  NMR spectra were recorded on a Bruker AVANCE III (Karlsruhe, Germany) at 400/100 MHz in  $\text{CDCl}_3$  or  $\text{DMSO}-d_6$ . Chemical shifts ( $\delta$ ) and coupling constants ( $J$ ) were reported in ppm and Hz, respectively. High resolution mass spectra (HRMS) were acquired with a Bruker microTOOF-Q II spectrometer. All reagents and ivermectin were commercially sourced and used as received without further purification.

### 3.2 General synthesis procedure for a1–a22

At room temperature, elemental sulfur (30.0 mmol) and NaOH (30.0 mmol) were added to a round-bottom flask, followed by 60 mL methanol. The mixture was stirred for 15 min, then substituted chalcone (10.0 mmol) was added, and the reaction was vigorously stirred for 72 h (monitored by TLC). After completion, the solid was collected *via* vacuum filtration, transferred to a beaker with 100 mL dichloromethane, sonicated for 10 min, and the filtrate was re-filtered. The filtrate solvent was removed by vacuum distillation, and the residue was recrystallized from ethyl acetate to yield tetrahydrothiophene derivatives (**a1–a22**, 32–91% yields).<sup>35</sup>

### 3.3 General synthesis procedure for b1–b22

At room temperature, newly synthesized tetrahydrothiophene derivative (3 mmol) was dissolved in 20 mL DCM. A preprepared 20 mL DCM solution of *m*-chloroperoxybenzoic acid (12.0 mmol) was then added dropwise, and the reaction was vigorously stirred for 6 h (monitored by TLC hourly until raw material was fully converted). After completion, excess solvent was removed by vacuum evaporation. The solid was washed with

a small amount of ethanol, and the residue was recrystallized from methanol to yield target products (**b1–b22**, 92–98% yields).

### 3.4 Acaricidal activity *in vitro*

The *in vitro* acaricidal activity of the synthesized tetrahydrothiophene derivatives against *Psoroptes cuniculi* was determined using the method previously established by our research group.<sup>36,37</sup> The specific operation was as follows. The test compound was dissolved in a mixed solvent (dimethyl sulfoxide: tween-80: physiological saline = 1:1:8, v:v:v) to prepare a test solution. 0.6 mL of the test solution was added to each well of a 24-well plate. Ten adult mites were inoculated into each well. Meanwhile, the mixed solvent without the test compound was set as the blank control, and the mixed solvent containing ivermectin was set as the reference control. Each compound was set with 6 parallel replicates. After incubating the 24-well plate at 28 °C under saturated humidity for 24 h, the number of dead mites in each well was recorded.

The mortality was calculated by the following formula:

$$\text{Mortality (\%)} = (N_{\text{test}} - N_{\text{blank}}) / (N_{\text{sample}} - N_{\text{blank}}) \times 100\%$$

For compounds in Table 2, gradient-concentration test solutions were prepared per the above procedure. Using probit values of average mortality and log concentrations, a concentration-effect toxicity regression equation was constructed to calculate  $\text{LC}_{50}$ . Similarly, these compounds were made into  $4.5\text{ }\mu\text{mol mL}^{-1}$  solutions. With probit values and log treatment times, a time-effect toxicity regression equation was established to obtain  $\text{LT}_{50}$ .

### 3.5 Molecular docking analysis

The 3D crystal structure of acetylcholinesterase (AChE, PDB ID: 5DTI) was retrieved from RCSB Protein Data Bank. Molecular docking of **b7**, **b16**, **b22** with AChE was conducted *via* Discovery Studio 2016 (Accelrys Inc., San Diego, USA). ChemBio 3D Ultra 14.0 built 3D models of target compounds, with hydrogenation optimization on AChE's crystal structure. The docking process followed our group's reported parameter scheme to ensure result reliability and repeatability.<sup>38</sup>

## 4 Conclusions

In summary, this study systematically developed tetrahydrothiophene derivatives, successfully preparing sulfone derivatives *via* oxidation. The synthesis process was characterized by easily available raw materials, simple post-treatment, and high yields. The results of *in vitro* acaricidal activity evaluation showed that when evaluated based on mass concentration and molar concentration, sixteen and fourteen compounds, respectively, exhibited significantly superior acaricidal activity to the commercially available benchmark drug ivermectin, demonstrating potent and rapid acaricidal efficacy. Structure–activity relationship (SAR) studies revealed that the sulfonyl group, as an essential structural unit for the acaricidal activity



of this class of compounds, can significantly enhance molecular activity when introduced. The introduction of halogens (F, Cl, Br) and strong electron-withdrawing groups ( $-\text{CF}_3$ ) at the *para* positions of the benzene rings at the 3- and 5-positions can significantly enhance activity. Molecular docking experiments further confirmed at the level of mechanism of action that tetrahydrothiophene sulfone derivatives can form multiple hydrogen bonds, halogen bonds, and  $\pi$ -type interactions with the active pocket of acetylcholinesterase (AChE), showing good targeted binding ability. This preliminarily clarified that they may exert acaricidal effects by inhibiting AChE. Therefore, the tetrahydrothiophene derivatives synthesized in this study, with their unique structural advantages, indicate great development potential in the field of mite control in agriculture and animal husbandry.

## Author contributions

Dongdong Chen designed the experiments and reviewed the manuscript. Yan Wang and Yujun Wu organized and analyzed the data. Qiaoqiao Yu, Yunhan Wang, Junyao Zheng, Zhong Ying and Changhui Hou prepared figures and SI.

## Conflicts of interest

There are no conflicts to declare.

## Data availability

CCDC 2468721 (b17) contains the supplementary crystallographic data for this paper.<sup>33</sup>

The data supporting this article have been included as part of the supplementary information (SI). Supplementary information is available. See DOI: <https://doi.org/10.1039/d5ra05421d>.

## Acknowledgements

This work was supported by the Key Research and Development Project of Lvliang (2024GX01) and Postgraduate Education Innovation Program of Shanxi Province (2025JG182).

## References

- 1 X. Shang, X. Guo, F. Yang, B. Li, H. Pan, X. Miao and J. Zhang, *Vet. Parasitol.*, 2017, **240**, 17–23.
- 2 T. V. Moskvina and L. V. Zheleznova, *Vet. Parasitol.: Reg. Stud. Rep.*, 2015, **1–2**, 31–34.
- 3 A. M. Hering, N. B. Chilton, T. Epp, H. M. Schwantje, F. Cassirer, A. Walker, C. McLean, P. R. Thampy, E. Hanak, P. Wolff, M. Drew, K. D. Bardsley and M. Woodbury, *Int. J. Parasitol.*, 2021, **14**, 273–279.
- 4 H. Wen, B. Pan, F. Wang, Z. Yang, Z. Wang, S. Liu and M. Wang, *Parasitol. Res.*, 2010, **106**, 607–613.
- 5 N. C. Romero, O. A. Flores, W. G. Sheinberg, C. A. Martin, J. E. Yarto, C. R. Heredia and G. L. G. Bautista, *PLoS One*, 2020, **15**, e0230753.
- 6 D. Engelman, K. Kiang, O. Chosidow, J. McCarthy, C. Fuller, P. Lammie, R. Hay and A. Steer, *PLoS Neglected Trop. Dis.*, 2013, **7**, e2167.
- 7 M. Kumar, B. Pal, R. D. Purkayastha and J. Roy, *J. Parasit. Dis.*, 2016, **40**, 41–45.
- 8 X. Shang, Y. Wang, X. Zhou, X. Guo, S. Dong, D. Wang, J. Zhang, H. Pan, Y. Zhang and X. Miao, *Vet. Parasitol.*, 2016, **226**, 93–96.
- 9 T. Ueda, H. Tarui, N. Kido, K. Imaizumi, K. Hikosaka, T. Abe, D. Minegishi, Y. Tada, M. Nakagawa, S. Tanaka, T. Omiya, K. Morikaku, M. Kawahara, T. Kikuchi-Ueda, T. Akuta and Y. Ono, *Genomics*, 2019, **111**, 1183–1191.
- 10 M. Lu, Y. Cai, S. Yang, Q. Wan and B. Pan, *Drug Dev. Ind. Pharm.*, 2018, **44**, 2000–2004.
- 11 C. Zhang, X. Gu, Y. Chen, R. Zhang, Y. Zhou, C. Huang, C. Wang, L. Xiong, Y. Xie, G. Yang, R. He, X. Zhou, D. Yang, B. Jing, X. Peng and Z. He, *Int. J. Biol. Macromol.*, 2021, **182**, 1399–1408.
- 12 R. R. D. Santos, C. N. Coelho, T. A. P. Batista, L. C. D. S. Nunes, T. R. Correia, F. B. Scott, A. G. V. Laguna and J. I. Fernandes, *Pesqui. Vet. Bras.*, 2017, **37**, 47–51.
- 13 K. Sharun, S. Anjana, S. A. Sidhique and S. Panikkassery, *J. Parasit. Dis.*, 2019, **43**, 733–736.
- 14 N. G. Uco Azamar, G. Arjona Jiménez, L. E. Cruz Bacab and H. E. De la Cruz Reyes, *Vet. Dermatol.*, 2024, **35**, 446–449.
- 15 G. Sheinberg, C. Romero, R. Heredia, M. Capulin, E. Yarto and J. Carpio, *Vet. Dermatol.*, 2017, **28**, 393–e91.
- 16 G. S. Sun, X. Xu, S. H. Jin, L. Lin and J. J. Zhang, *Molecules*, 2017, **22**, 958.
- 17 X. F. Shang, X. L. Miao, L. X. Dai, Y. Wang, B. Li, H. Pan and J. Y. Zhang, *Vet. Parasitol.*, 2021, **296**, 109498.
- 18 K. Bozorov, L. F. Nie, J. Zhao and H. A. Aisa, *Eur. J. Med. Chem.*, 2017, **140**, 465–493.
- 19 R. Mishra, N. Sachan, N. Kumar, I. Mishra, P. Chand and J. Heterocyclic, *Chem*, 2018, **55**, 2019–2034.
- 20 Y. N. Wu, R. Fu, N. N. Wang, W. J. Hao, G. Li, S. J. Tu and B. Jiang, *J. Org. Chem.*, 2016, **81**, 4762–4770.
- 21 N. Winter, Z. Rupcic, M. Stadler and D. Trauner, *J. Antibiot.*, 2019, **72**, 375–383.
- 22 S. Shi, P. Zhang, C. Luo, S. Zhuo, Y. Zhang, G. Tang and Y. Zhao, *Org. Lett.*, 2020, **22**, 1760–1764.
- 23 D. Sung, B. Mun, S. Park, H. Lee, J. Lee, Y. Lee, H. J. Shin and J. S. Lee, *J. Org. Chem.*, 2019, **84**, 379–391.
- 24 M. E. Boursier, J. B. Combs and H. E. Blackwell, *ACS Chem. Biol.*, 2019, **14**, 186–191.
- 25 L. Lu, J. Chen, W. Tao, Z. Wang, D. Liu, J. Zhou, X. Wu, H. Sun, W. Li, G. Tanabe, O. Muraoka, B. Zhao, L. Wu and W. Xie, *J. Med. Chem.*, 2023, **66**, 3484–3498.
- 26 P. Lv, Y. Chen, Z. Zhao, T. Shi, X. Wu, J. Xue, Q. X. Li and R. Hua, *J. Agric. Food Chem.*, 2018, **66**, 1023–1032.
- 27 S. Mohan, K. Jayakanthan, R. Nasi, D. A. Kuntz, D. R. Rose and B. M. Pinto, *Org. Lett.*, 2010, **12**, 1088–1091.
- 28 G. R. Bommineni, K. Kapilashrami, J. E. Cummings, Y. Lu, S. E. Knudson, C. Gu, S. G. Walker, R. A. Slayden and P. J. Tonge, *J. Med. Chem.*, 2016, **59**, 5377–5390.
- 29 E. Block, B. Dethier, B. Bechand, J. J. Cotelesage, G. N. George, K. Goto, I. J. Pickering, E. Mendoza Rengifo,





- R. Sheridan, E. Y. Sneed and L. Vogt, *J. Agric. Food Chem.*, 2018, **66**, 10193–10204.
- 30 K. Calabro, L. K. Jennings, P. Lasserre, R. Doohan, D. Rodrigues, F. Reyes, C. Ramos and O. P. Thomas, *J. Org. Chem.*, 2020, **85**, 14026–14041.
- 31 H. V. Le, D. D. Hawker, R. Wu, E. Doud, J. Widom, R. Sanishvili, D. Liu, N. L. Kelleher and R. B. Silverman, *J. Am. Chem. Soc.*, 2015, **137**, 4525–4533.
- 32 M. Tian, X. Wang, G. Tang, G. Cui, J. Zhou, J. Jin and B. Xu, *ACS Med. Chem. Lett.*, 2025, **16**, 101–108.
- 33 CCDC 2468721 (**b17**): Experimental Crystal Structure Determination, 2025, DOI: [10.5517/ccdc.csd.cc2nvx5m](https://doi.org/10.5517/ccdc.csd.cc2nvx5m).
- 34 L. Dai, X. Miao, B. Li, J. Zhang, H. Pan and X. Shang, *Vet. Parasitol.*, 2020, **286**, 109247.
- 35 D. Chen, Y. Bai, Q. Cheng, J. Li, Z. Tong, J. Hou, T. Liu, Y. Guo, X. Tang, X. Yang and X. Yang, *Arabian J. Chem.*, 2022, **15**, 104097.
- 36 D. Chen, Y. Tian, M. Xu, X. Wang, D. Li, F. Miao, X. Yang and L. Zhou, *Sci. Rep.*, 2018, **8**, 1797.
- 37 D. D. Chen, B. Y. Zhang, X. X. Liu, X. Q. Li, X. J. Yang and L. Zhou, *Bioorg. Med. Chem. Lett.*, 2018, **28**, 1149–1153.
- 38 D. Chen, Y. Cheng, L. Shi, X. Gao, Y. Huang and Z. Du, *Molecules*, 2024, **29**, 41243.

